Regenerative Therapy 14 (2020) 284–295

Contents lists available at ScienceDirect

Regenerative Therapy

journal homepage: http://www.elsevier.com/locate/reth

Original Article

Optimization of culture duration of bone marrow cells before transplantation with a β-tricalcium phosphate/recombinant collagen peptide hybrid scaffold

Ryo Umeyama [a], Takanori Yamawaki [a], Dan Liu [a], Sanshiro Kanazawa [a], Tsuyoshi Takato [b], Kazuto Hoshi [a, c], Atsuhiko Hikita [c, *]

[a] Department of Sensory and Motor System Medicine, Department of Oral-maxillofacial Surgery, Dentistry and Orthodontics, Graduate School of Medicine, The University of Tokyo, Hongo 7-3-1, Bunkyo-ku, Tokyo 113-8655, Japan
[b] JR Tokyo General Hospital, 2-1-3 Yoyogi, Shibuya, Tokyo 151-8528
[c] Department of Cell & Tissue Engineering (FUJISOFT), Division of Tissue Engineering, The University of Tokyo Hospital, Hongo 7-3-1, Bunkyo-ku, Tokyo 113-8655, Japan

ARTICLE INFO

Article history:
Received 20 February 2020
Received in revised form
15 March 2020
Accepted 4 April 2020

Keywords:
Bone regeneration
Osteoblast
Recombinant collagen peptide
3D printing
Bone marrow cells

ABSTRACT

Introduction: Currently, various kinds of materials are used for the treatment of bone defects. In general, these materials have a problem of formativeness. The three -dimensional (3D) printing technique has been introduced to fabricate artificial bone with arbitrary shapes, but poor bone replacement is still problematic. Our group has created a β-tricalcium phosphate (β-TCP) scaffold by applying 3D printing technology. This scaffold has an arbitrary shape and an internal structure suitable for cell loading, growth, and colonization. The scaffold was coated with a recombinant collagen peptide (RCP) to promote bone replacement. As indicated by several studies, cells loaded to scaffolds promote bone regeneration, especially when they are induced osteoblastic differentiation before transplantation. In this study, culture duration for bone marrow cells was optimized before being loaded to this new scaffold material.

Method: Bone marrow cells isolated from C57BL/6J mice were subjected to osteogenic culture for 4, 7, and 14 days. The differentiation status of the cells was examined by alkaline phosphatase staining, alizarin red staining, and real-time RT-PCR for differentiation markers. In addition, the flow of changes in the abundance of endothelial cells and monocytes was analyzed by flow cytometry according to the culture period of bone marrow cells.

Next, cells at days 4, 7, and 14 of culture were placed on a β-TCP/RCP scaffold and implanted subcutaneously into the back of C57BL/6J mice. Grafts were harvested and evaluated histologically 8 weeks later. Finally, Cells cultured for 7 days were also transplanted subperiosteally in the skull of the mouse with scaffolds.

Result: Alkaline phosphatase staining was most prominent at 7 days, and alizarin red staining was positive at 14 days. Real-time RT-PCR revealed that *Runx2* and *Alp* peaked at 7 days, while expression of *Col1a1* and *Bglap* was highest at 14 days. Flow cytometry indicated that endothelial cells increased from day 0 to day 7, while monocytes increased continuously from day 0 to day 14. When transplanted into mice, the scaffold with cells cultured for 7 days exhibited the most prominent osteogenesis. The scaffold, which was transplanted subperiosteally in the skull, retained its shape and was replaced with regenerated bone over a large area of the field of view.

Conclusion: Osteoblasts before full maturation are most efficient for bone regeneration, and the preculture period suitable for cells to be loaded onto a β-TCP/RCP hybrid scaffold is approximately 7 days. This β-TCP/RCP hybrid scaffolds will also be useful for bone augmentation.

* Corresponding author. Atsuhiko Hikita: Department of Cell & Tissue Engineering (FUJISOFT), Division of Tissue Engineering , The University of Tokyo Hospital, Hongo 7-3-1, Bunkyo-ku, Tokyo 113-8655, Japan.
E-mail address: ahikita-tky@umin.ac.jp (A. Hikita).
Peer review under responsibility of the Japanese Society for Regenerative Medicine.

https://doi.org/10.1016/j.reth.2020.04.005

1. Introduction

Bone is important as a supporting tissue of the body. Loss of bone leads to a major decrease in quality of life [1,2]. In the oral and maxillofacial region, periodontitis, tumors, cysts, and congenital anomalies are the main causes of bone loss, and treatment is performed to regenerate the lost bone, and use the regenerated bone as a foundation for subsequent prosthetic treatment [3–5].

Currently, transplantation of autologous bone such as particulate cancellous bone and marrow (PCBM) is the gold standard for the treatment of bone defects. However, the use of autogenous bone has problems such as increased surgical invasiveness, and limited collection volume [6,7]. Drugs such as porcine enamel matrix protein and other biologically-derived preparations [8,9] have also been used, but are not enough for recovery from large bone defects. Collagen sponges are also used, while its low osteoinductive ability and low mechanical strength of the material make it difficult to use it at the load-bearing site [10,11]. In addition, use of these xenogeneic materials may cause unknown infectious diseases and provoke religious issues. On the other hand, artificial bone made of ceramic materials such as hydroxyapatite [12,13] and β-tricalcium phosphate (β-TCP) has excellent mechanical strength and osteoconductivity, and is often used as a substitute for autologous bone. However, it lacks osteoinductive ability and low bioabsorbability, making it difficult to obtain bone regeneration equivalent to autologous bone [14,15].

In addition, it is difficult to provide an arbitrary shape to these artificial bones. One solution to the problem of formativeness is a 3D printing technique that has been developed with the advancement of computer technology [16–18]. Our group reported the development of an artificial bone using a 3D printer [19–21]. The artificial bone fabricated by laminated printing can be made into a shape suitable for bone defects, which enables a good aesthetic outcome of surgery. However, this artificial bone shows a very slow rate of bone replacement, which is attributable to the lack of endogenous structures for cell invasion or retention, or low biodegradability [20].

The use of collagen as a scaffolding material enables the activation of various mechanisms that promote organization and calcification, and allows the formation of regenerated bone with the composition and morphological characteristics of the endogenous bone [22–24]. Furthermore, the addition of collagen to the β-TCP scaffold increases cell adhesion, proliferation, and matrix synthesis in vitro [25,26] and bone regeneration *in vivo* [27,28]. However, the quality and purity of collagen derived from animal tissue are uneven. In addition, xenogeneic materials have the risk of infection by contamination with non-human proteins or pathogenic materials, and the risk of immune responses [29].

To overcome these shortcomings, recombinant collagen peptide (RCP) is used to modify the scaffold surface. The arginine-glycine-aspartate (RGD) peptide has been shown to promote osteoblast proliferation, differentiation, and mineralization [30].

Considering these circumstances, we developed a new scaffold for bone regeneration. The scaffold possesses continuous holes to inject cells and to induce the migration of host cells, which induces bone regeneration and scaffold degradation. In addition, the scaffold is coated by the RCP developed by Fujifilm Corporation (Cell Nest). Cell Nest is rich in the RGD motif, which binds to integrins and other cell adhesion molecules [31]. Cell Nest is xeno-free and has high processability and stable production quality [32,33].

In addition, a previous report indicated that bone regeneration is more effective when scaffolds are loaded with bone marrow cells pre-cultured under an osteogenic condition [34]. Therefore, to achieve efficient bone regeneration, we envisioned the use of this hybrid scaffold material with bone marrow cells subjected to bone differentiation culture.

Here, we optimized the culture period of bone marrow cells seeded on the hybrid scaffold. Bone marrow-derived cells were differentiated for 4, 7, and 14 days to evaluate the relation between the degree of in vitro differentiation and *in vivo* osteogenic potential, and to determine the appropriate culture period. Furthermore, bone regeneration in a bone augmentation model was evaluated.

2. Material and methods

2.1. Approval for animal experiments

All animal experiments were approved by the University of Tokyo (#P15-091) and conducted according to the Act on the Welfare and Management of Animals and the Standards Relating to the Care and Keeping and Reducing Pain of Laboratory Animals (Notice of the Ministry of the Environment), the Guidelines for Animal Experiments at the Faculty of Medicine, the University of Tokyo, and the ARRIVE Guidelines.

2.2. β-TCP/RCP hybrid scaffold

The β-TCP/RCP hybrid scaffold possessing continuous holes was created in cooperation with Fujifilm Corporation (Fig. 1 a-c).

2.2.1. Ink

After preparing citric acid (anhydrous) and trisodium citrate dihydrate as 1.2M aqueous solution using distilled water independently, the same amounts of both aqueous solutions were mixed, and the pH was confirmed to be about 3.05.

2.2.2. Powder

Spherical-shaped tetracalcium phosphate (TTCP) particles and plate-shaped dicalcium hydrogen phosphate dihydrate (DCPD) particles were mixed at a ratio of 1 mol:2 mol of TTCP: DCPD.

2.2.3. Shaping

The basic structure of the scaffold was fabricated by ZPrinter 310 Plus (Z Corporation, Rock Hill, SC, United States) using the powder and the ink described above. The stacking height of one layer was set to 100 μm. The molding was sintered in a muffle furnace at 1100 °C for 2 h.

2.2.4. RCP coating

A 7wt% aqueous solution of RCP was warmed to 40 °C and the fabricated material was immersed. The material was then placed in a vacuum desiccator, in which the air pressure was reduced to −0.09 MPa and returned to atmospheric pressure. The process was repeated three times or more, and the molded material was subjected to thermal crosslinking at 148 °C for about 4 h.

2.3. Evaluation of the properties of the scaffold

The density of the scaffold was measured by Archimedes' method. For the longitudinal compression breakage test of the scaffold, we used MX2 and digital force gauge ZTA-1000N. The composition of the scaffold was analyzed using the X-ray diffraction method. The porosity of the scaffold was evaluated by the Hg indentation method. The penetration rate of the aqueous solution into the scaffold was measured for the time to penetrate to a height of 15 mm by soaking the ink from the bottom.

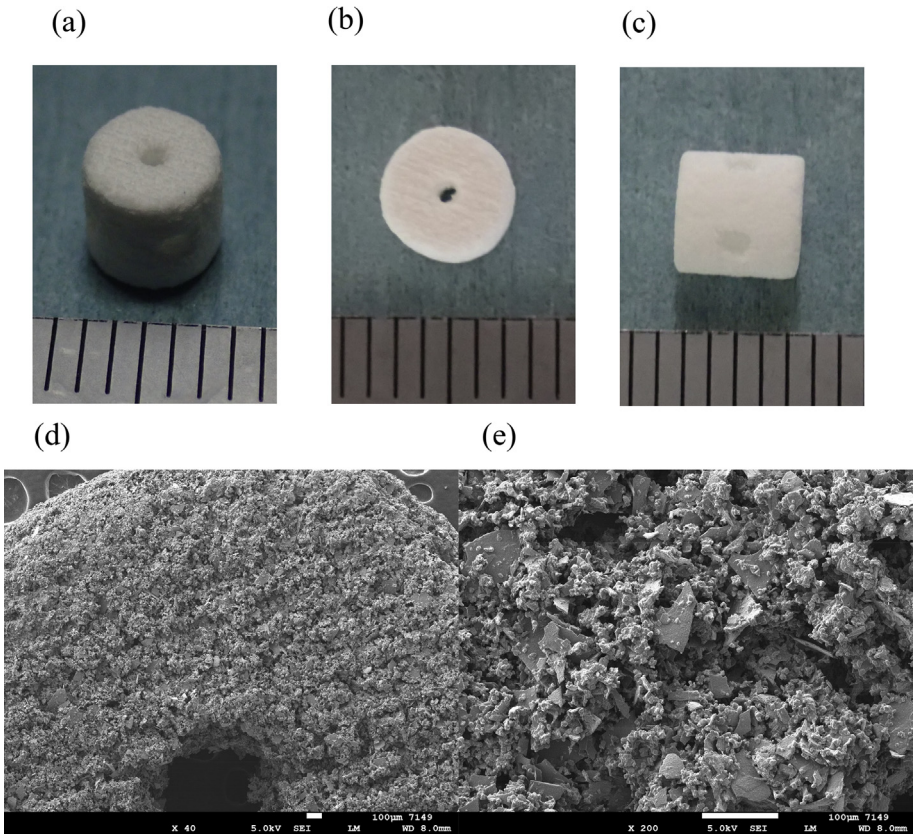

Fig. 1. (a–c) Macroscopic view of β-TCP/RCP hybrid scaffold. The scaffold has a cylindrical shape with a diameter of 5 mm and a height of 5 mm(d–e) SEM images of β-TCP/RCP scaffold. The magnification of (d) is × 40 and (e) is × 200. Scale bars indicate 100 μm.

2.4. Scanning electron microscopy (SEM)

The samples were fixed with phosphate-buffered 2% glutaraldehyde followed by immobilization with 2% osmium triacetic acid for 2 h on ice. The samples were then dehydrated in stepwise ethanol and dried by lyophilization with t-butyl alcohol. The dried specimens were coated with an osmium plasma ion coater, and SEM observation was carried out at 5 kVat using JSM-7500F (JEOL, Tokyo, Japan).

2.5. Isolation and culture of mouse bone marrow cells

Six-week-old male C57BL/6J mice (CLEA Japan Inc. Tokyo, Japan) were euthanized by cervical dislocation. Iliac bone, femur, and tibia were harvested using forceps and scissors. Bones were crushed with a pestle and further chopped with forceps for 6 min. Bone fragments were washed 5 times with 5 ml of Hanks' Balance Salt Solution (HBSS (−)) with phenol red, 1% penicillin/streptomycin (Sigma-Aldrich Co., MO, USA), 1% 4-(2-hydroxyethyl)-1-piperazineethanesulfonic acid (Gibco Life Technologies, Carlsbad, CA, USA), and 2% fetal bovine serum (FBS) (Gibco Life Technologies, Carlsbad, CA,USA). The collected bone marrow fluid was passed through a cell strainer with a pore size of 70 μl to remove the bone debris and centrifuged at 1500 rpm for 5 min. For the lysis of erythrocytes, 1 ml of sterile water was added to the cell pellet and stirred for 6 s, followed by the addition of 1 ml of 2 x phosphate-buffered saline (PBS) and 8 ml of HBSS. The agglomerates formed by these procedures were removed through a 70-μm cell strainer (BD Falcon, Bedford, MA, USA), and the cell suspension was centrifuged at 1500 rpm for 5 min. Cells were resuspended with 6 ml of cell growth medium: IMDM (Gibco Gibco Life Technologies, Carlsbad, CA, USA) supplemented with 20% FBS, 20 ng/ml FGF2 (Kaken Pharmaceutical Co, Ltd. Tokyo, Japan), and 1% penicillin/streptomycin.

One milliliter of cell suspension was seeded into 1 well of a six-well plate for transplantation, 1 ml was placed in a 100-mm tissue culture dish for real-time RT-PCR, and 0.2 ml was seeded into 1 well of a 24-well plate for cell staining, and incubated in a 37 °C 5% CO2 incubator. After 24 h, half of the medium was exchanged for osteoblast differentiation induction medium: RPMI 1640 (Sigma-Aldrich, St. Louis, MO, USA) supplemented with 20% FBS, 1% penicillin/streptomycin, and osteoblast-inducer reagent (for animal cell) (Takara-bio Inc. Shiga, Japan). After another 24 h, the entire medium was replaced with osteoblast differentiation induction medium, and the medium was changed once every 2 days thereafter (Fig. 2). Control wells were also prepared for cell staining, in which growth medium alone was used.

2.6. Cell staining

Cells cultured for 4, 7, and 14 days were used for cell staining. After removal of the medium, each well was washed twice with 1 ml of PBS. Then, 0.5 ml/well of 4% paraformaldehyde phosphate buffer solution, which had been pre-cooled, was added and incubated for 10 min on ice to fix the cells. Subsequently, the fixative was diluted with 2 ml of PBS and removed, and each well was washed twice with PBS.

Alkaline phosphatase staining was performed using the TRACP & ALP Double-stain Kit (Fujifilm wako, Tokyo, Japan) according to the protocol provided by the manufacturer. Subsequently, 250 μl of alkaline phosphatase premix substrate solution was added to the wells, and cells were incubated at 37 °C for 15 min.

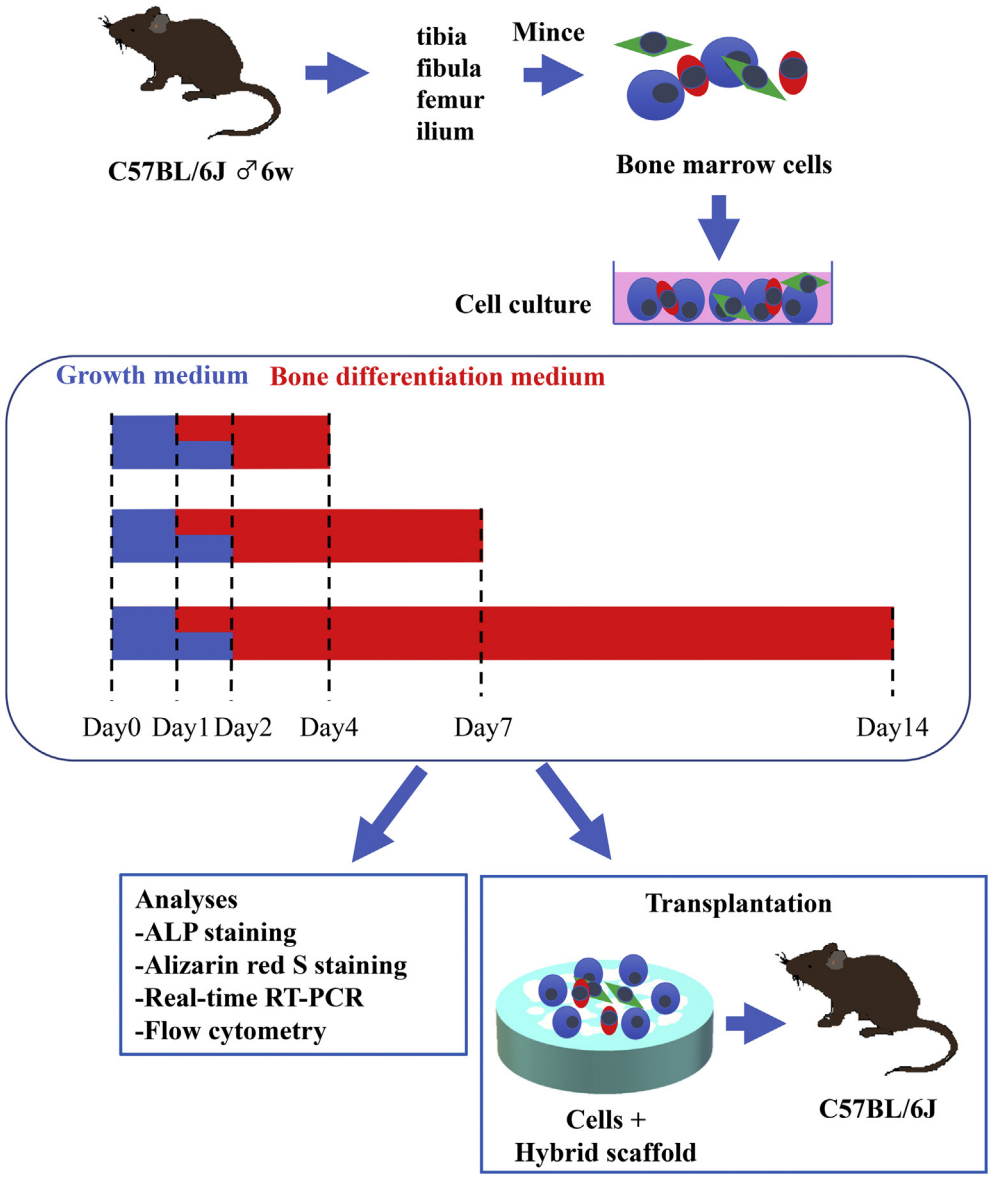

Fig. 2. Scheme of cell collection and culture.

Alizarin red S staining was performed by adding 250 μl of alizarin red S solution to the wells. After incubation at 37 °C for 15 min, each well was washed three times with distilled water.

The plates were then inverted and dried followed by observation by phase-contrast microscopy. The stained areas were quantified and confirmed using Image J [35,36].

2.7. Real-time RT-PCR

Total RNA was extracted from cells using ISOGEN II (Nippon Gene, Toyama, Japan) according to the manufacturer's protocol. Briefly, 200 μl of distilled, deionized, sterile water (Nippon Gene, Toyama, Japan) was added to 1000 μl of the cell lysate harvested with ISOGEN II. After centrifugation (12,000×*g*, 15 min, 4 °C) of the solution, the aqueous phase containing RNA was collected. The aqueous solution was mixed with 500 μl of isopropanol and centrifuged (12,000×*g*, 10 min) to make the precipitate. Next, 1000 μl of 75% ethanol was added to the precipitate, and the solution was centrifuged (7500×*g*, 5 min). The pellet was air-dried and dissolved in distilled, deionized, sterile water. The total RNA obtained was reverse transcribed with SuperScript IV Reverse Transcriptase (Life Technologies, Carlsbad, CA, USA) to produce cDNA. Gene expression was measured using a 7500 Fast Real-time PCR System (Applied BioSystems, Carlsbad, CA, USA). The expression level of the target gene was corrected using *Gapdh* as an internal standard. The ΔΔCt method was used for the analysis. Target genes were *Runx2* and *Col1a1* as markers at the early stage of differentiation, *Alp* as a marker at the mid stage of differentiation, and *Bglap* as a marker at the late stage of differentiation [37,38]. Primers with detectable sequences of the target gene were designed as shown in Table 1. Gene expression in cells cultured for 4, 7, and 14 days was examined by real-time RT-PCR (N = 3).

2.8. Flow cytometry

The flow of changes in the abundance of endothelial cells and monocytes was analyzed by flow cytometry according to the culture period of bone marrow cells (Fig. 6). After isolation of cells,

Table 1
Primers for real-time RT-PCR.

Primer	Forward Primer	Reverse Primer
Runx2	5′-CGGTCTCCTTCCAGGATGGT-3′	5′-GCTTCCGTCAGCGTCAACA-3′
Col1a1	5′-AACCCGAGGTATGCTTGATCT-3′	5′-CCAGTTCTTCATTGCATTGC-3′
Alp	5′-GTTGCCAAGCTGGGAAGAACAC-3′	5′-CCCACCCCGCTATTCCAAAC-3′
Ocn	5′-GGGAGACAACAGGGAGGAAA-3′	5′-CAGGCTTCCTGCCAGTACCT-3′
Gapdh	5′-GTTGTCTCCTGCGACTTCA-3′	5′-GGTGGTCCAGGGTTTCITA-3′

cells cultured for 4, 7 and 14 days were used for analysis. Cells cultured in a 6-well plate was washed twice with PBS, 1 ml of Trypsin-EDTA solution (Sigma-Aldrich, St. Louis, MO, USA) was added, and allowed to stand for 15 min at 37 °C. Cells were detached by tapping and collected. The collected cells were suspended in 1 ml of HBSS and analyzed. To a tube, TruStain fcX ™ (anti-mouse CD16/32) Antibody (BioLegend, San Diego, CA, USA) was added at a concentration of 2 μg/100 μl, and the mixture was incubated on ice for 10 min to block the Fc portion. Thereafter, the cells were stained using antibodies against surface markers. Table 2 shows the antibodies used.

And Table 3 shows the antibodies used as isotype controls. After adding the antibody, the mixture was incubated on ice for 30 min in the dark. Thereafter, 500 μl of HBSS was added, and the mixture was centrifuged at 1500 rpm for 5 min. After the removal of the supernatant, DAPI was added to label dead cells. Cells were resuspended in HBSS, and analyzed using BD FACS Aria Fusion (BD Falcon, Bedford, Mass., USA). Monocytes were indicated as CD14 and CD45 double positive cells [39], and vascular endothelial cells as CD31 and CD144 double positive cells [40].

2.9. Transplantation of cells loaded into the β-TCP/RCP hybrid scaffold

Cells in each well of a 6-well plate were collected by incubation with 1 ml of trypsin-EDTA solution (Sigma-Aldrich, St. Louis, MO, USA) at 37 °C for 15 min on days 4, 7, or 14 of culture and then resuspended in cell growth medium at the concentration of 3.5×10^5 cells/35 μl.

C57BL/6J mice were given general anesthesia with isoflurane, and skin was incised on the shoulders and the lumbar region, one on each side, to create four subcutaneous pockets. Subsequently, hybrid scaffolds were loaded with cells and transplanted into the pockets together with non-cell-seeded hybrid scaffolds as controls. The implanted scaffolds were collected after 8 weeks.

2.10. Histological analysis

The harvested tissues were fixed with 4% paraformaldehyde phosphate buffer solution overnight. The tissues were demineralized by immersion in double-diluted K-CX (Falma, Osaka, Japan) for 1 week. The decalcified tissues were embedded in paraffin and sectioned with a microtome to a thickness of 0.5 μm. After deparaffinization, tissue sections were stained with hematoxylin and eosin and mounted using Mount Quick (COSMO BIO Co., Ltd., Tokyo, Japan).

Thereafter, 3 regions of interest (ROI) of a 20-fold field of view of the phase contrast microscope were set at 3 places on the left, center, and right of all samples, and images were captured. Each image was binarized using Image J, and the HE staining positive area (%) in single image was calculated. The average value per sample in control group or each group loaded with cells cultured for 4, 7, and 14 days was calculated from the 3 ROI images. The average of the 3 control samples (background) was subtracted from each value of cell-loaded group, and the average of the 3 samples was calculated (Fig. 7e).

2.11. Subperiosteal transplantation of scaffold loaded with the cells

A scaffold loaded with cells from culture of 7 days was prepared as described above, and implanted subperiosteally in the skull. After general anesthesia of C57BL/6J mice using isoflurane, a transverse incision was made with a scalpel behind the pinna, and the skin and periosteum were peeled with a scalpel and a spatula to the front of the skull to indicate bregma (point of intersection with the sagittal suture and coronal suture). The cell-loaded scaffold was placed on bregma and the skin and occipital muscles were sutured with 5–0 nylon thread. The transplanted scaffold was harvested by skin incision 8 weeks later (N = 3).

2.12. Statistical analysis

Statistical analysis was performed by ANOVA test. $P < 0.05$ was considered statistically significant.

3. Results

3.1. Properties of scaffolds

The density of the scaffold analyzed by Archimedes' principle was 880 kg/m^3. The mechanical strength of this scaffold was 2.4 ± 0.6 MPa. In X-ray diffraction, the mass fraction ratio of β-TCP

Table 2
List of antibodies used in Flowcytometry.

	Lot
Monocyte	
CD14 FITC Rat Anti-Mouse CD14 BD Bioscience, Bedford, MA, USA	6133796
CD45 APC-Cy-7 Rat Anti-Mouse CD45 BD Bioscience, Bedford, MA, USA	8222690
Endothelium	
CD31 PE-Cy7 Rat Anti-Mouse CD31 BD Bioscience, Bedford, MA, USA	8192872
CD144 PE Rat Anti-Mouse CD144 BD Bioscience, Bedford, MA, USA	8215572

Table 3
List of Isotype Control antibodies used in Flowcytometry.

	Lot
Monocyte	
CD14 FITC conjugated Rat IgG1, k, Isotype Control BD Bioscience, Bedford, MA, USA	553924
CD45 APC-Cy7 conjugated Rat IgG2b, k, Isotype Control BD Bioscience, Bedford, MA, USA	552773
Endothelium	
CD31 PE-Cy7 Rat Anti-Mouse CD31 BD Bioscience, Bedford, MA, USA	561410
CD144 PE conjugated Rat IgG2a, k, Isotype Control BD Bioscience, Bedford, MA, USA	553930

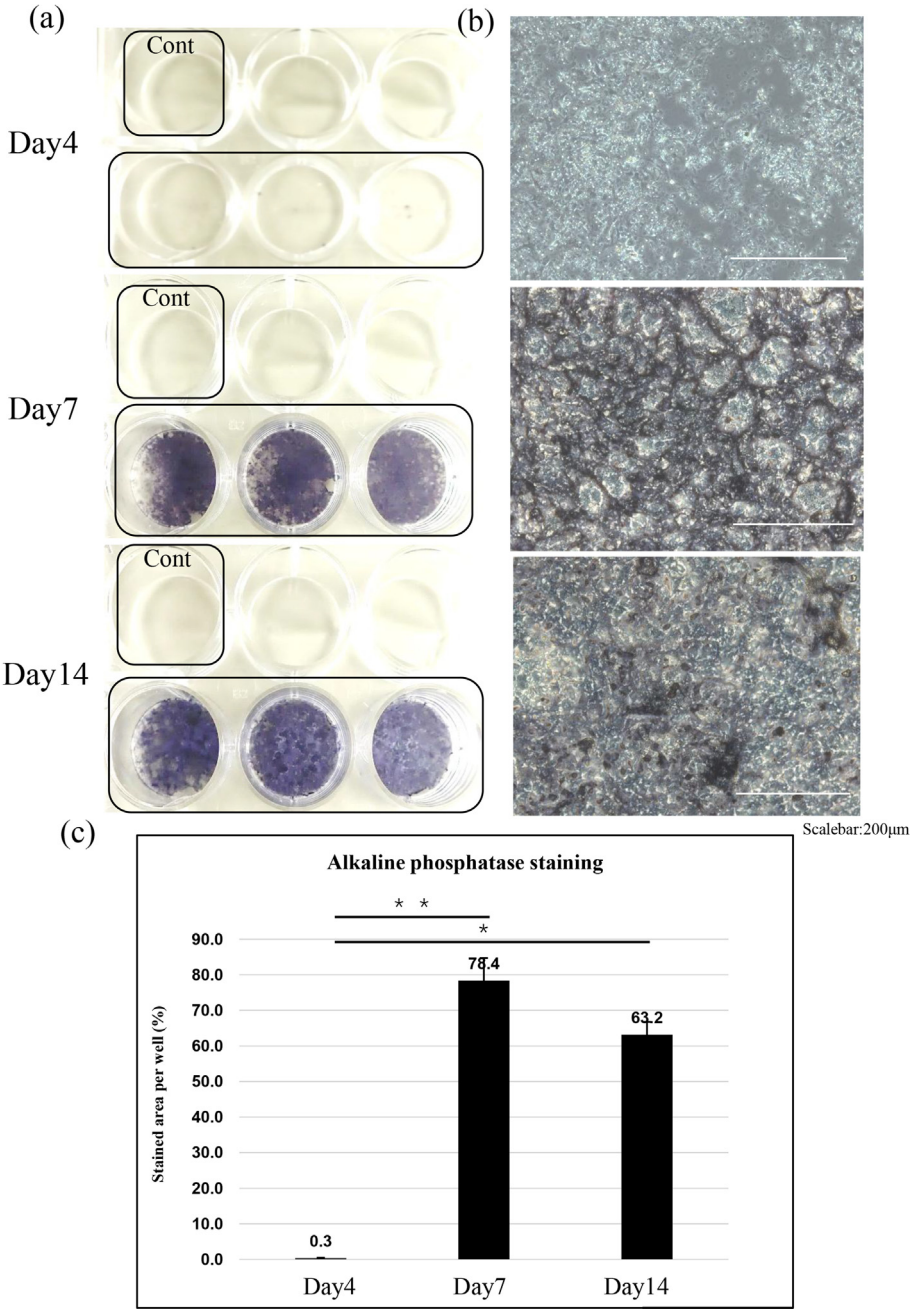

Fig. 3. Alkaline phosphatase staining. (a) Macroscopic pictures of a stained plate. The upper left well of each plate indicates the control well. Cont: a control well in which bone differentiation was not induced. (b) The phase contrast micrograph of the stained cells. Scale bars indicate 200 μm. (c) Quantification of the stained area using Image J. *p < 0.05, **p < 0.01. Error bars; mean ± S. D.

to the whole was 80% (±5%). The porosity was 65% ± 5%. The permeability of water was 1.0 ± 0.4 mm/s.

3.2. SEM observation

The surface properties and the detailed structure of this scaffold were examined by SEM. SEM microphotographs revealed a rough surface structure of this scaffold and layered pattern of β-TCP at × 40 (Fig. 1d). Plate-shaped and spherical-shaped β-TCPs and a pore structure between β-TCPs were observed at × 200 (Fig. 1e). SEM observations at × 40 and × 200 showed the presence of various sizes of β-TCP granules. RCP under the resolution limit could not be observed. The longitudinal diameter of the plate-shaped β-TCP observed on the surface was 59 μm on an average of 10 particles (Fig. 1d and e).

3.3. Cell staining

Mouse bone marrow cells were cultured in osteoblast differentiation induction medium for 4, 7, and 14 days. Alkaline phosphatase and alizarin red S staining were performed to analyze the changes in the degree of differentiation of the cells during the in vitro culture period. Alkaline phosphatase activity was observed on day 4 of culture, increased up to day 7, and slightly decreased at day 14 (Fig. 3a and b). Semi-quantitative analysis showed that alkaline phosphatase activity levels of day 7 and day 14 were significantly

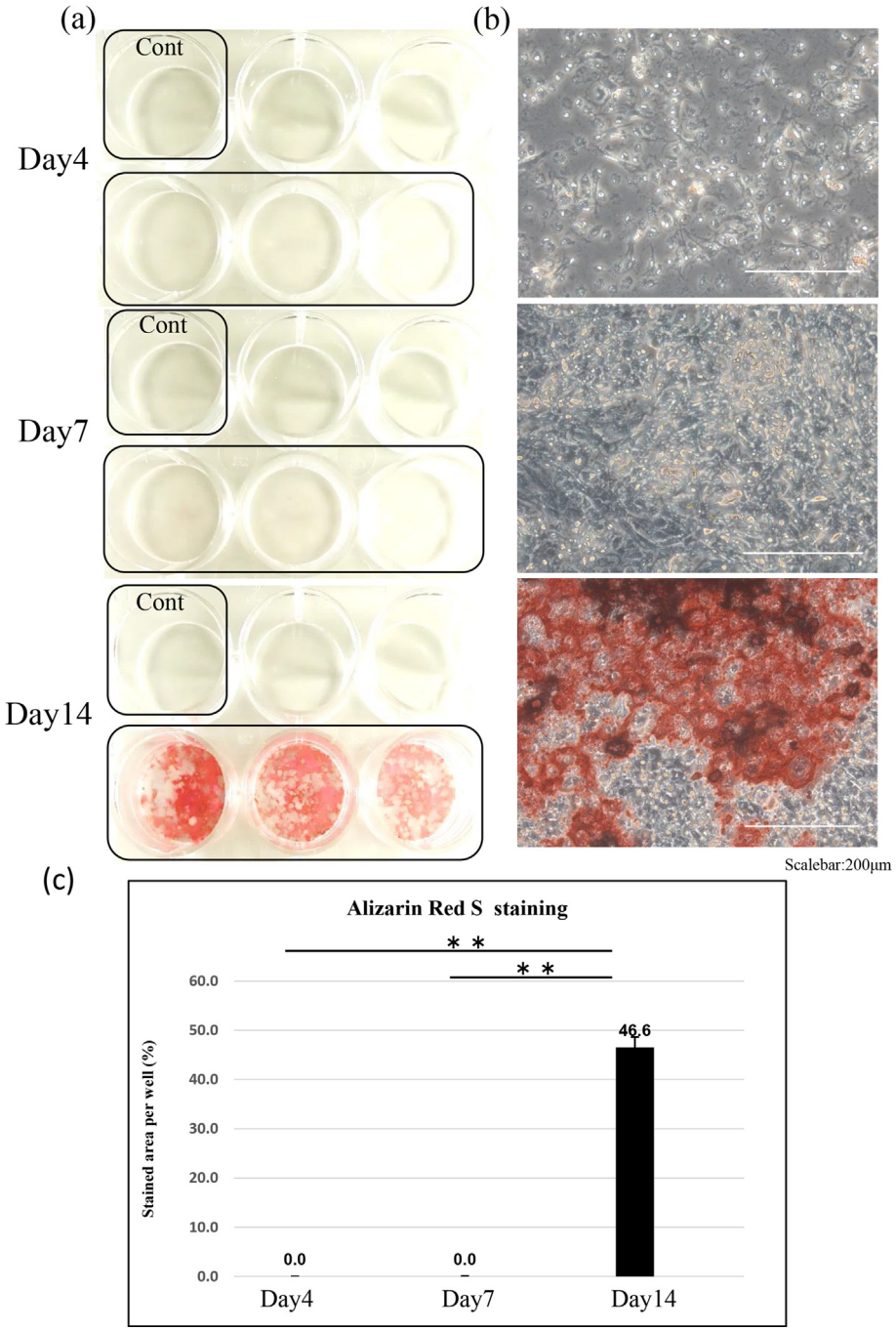

Fig. 4. Alizarin red S staining. (a)Macroscopic picture of a stained plate. The upper left well of each plate indicates the control well. (b) The phase contrast micrograph of the stained cells. Scale bars indicate 200 μm. (c) Quantification of the stained area using Image J. *p < 0.05, **p < 0.01. Error bars; mean ± S. D.

higher than that of day 4, while no significant difference was found between those of day 7 and day 14 (Fig. 3c). Alizarin red S staining showed substrate formation on day 14 of culture (Fig. 4a and b). The alizarin red S-stained area at day 14 was significantly larger than those of day 4 and day 7 (Fig. 4c). These results confirmed that as the culture period progressed, osteoblasts in bone marrow cells differentiated and produced bone matrix on day 14.

3.4. Real-time RT-PCR

In order to examine the degree of differentiation of osteoblasts at each stage in more detail, the expression of differentiation markers was analyzed by real-time RT-PCR. Expression of *Runx2*, a marker in the early stage of differentiation, was significantly higher at day 7 than at day 4 and day 14. Relative expression of *Col1a1* significantly increased on day 14. The expression of *Alp*, a marker of metaphase differentiation, was about 123 times higher from day 4 to day 7 of culture with a significant difference and tended to decrease slightly on day 14. The expression of *Bglap*, known as a late differentiation marker, predominantly increased over time (Fig. 5a–d). These results confirmed that differentiation markers of osteoblasts changed according to the culture period, and different cell populations could be collected depending on the culture period.

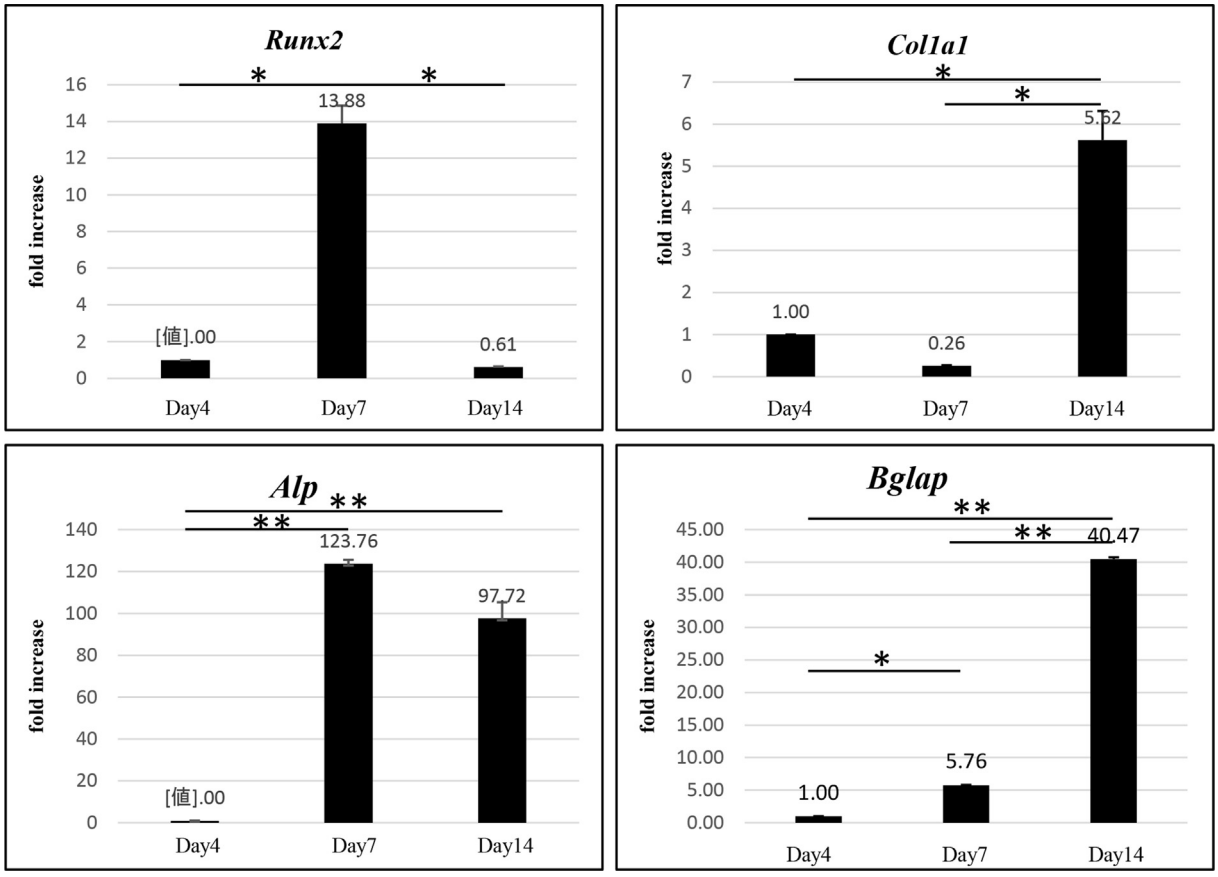

Fig. 5. Expression of differentiation markers. Real-time RT-PCR (ΔΔCt method) of osteogenic differentiation markers (*Runx2, Col1a1, Alp, Bglap*). *p < 0.05, **p < 0.01. Error bars; mean ± S. D.

3.5. Changes in the abundance of endothelial cells and monocytes during the culture period of bone marrow cells

The endothelial cells increased significantly ($p < 0.01$) between day 0 and day4, and day 4 and day 7, while no increase was observed between days 7 and 14 of the culture (Fig. 6a). Monocytes increased significantly ($p < 0.01$) between day 0 and day 4, day 4 and day 7, and day 7 and day 14 of culture (Fig. 6b).

3.6. Transplantation of cells with scaffolds

To investigate the effect of different culture periods on bone formation after transplantation, scaffolds seeded with cells at each stage were implanted subcutaneously in the back of mice (Fig. 7a–d). In the non-cell-loaded hybrid scaffold group, as a negative control, bone replacement was hardly detected (Fig. 7a). The day 4 group showed partial bone regeneration, while most of the scaffold remained without regenerated bone (Fig. 7b). On the other hand, the hybrid scaffold was replaced with new (regenerative) bone (NB) in a relatively larger area in the day 7 group. Many cells were found in the scaffold, and regenerative bone was seen in the space between the scaffold materials. In addition, circular translucent regions were observed, suggesting the existence of adipocytes (Fig. 7c). In the day 14 group, the hybrid scaffold was rarely replaced with NB, and most of the scaffold remained (Fig. 7d). In the quantification analysis, the HE positive area increased significantly ($p < 0.01$) from day 4 to day 7 (Fig. 7e). These findings suggested that in vitro bone regeneration was best achieved by seeding cells at 7 days of culture.

3.7. Transplantation of scaffold loaded with the optimized cells subperiosteally in the mouse skull

Using a bone augmentation model, bone regeneration under the pressure from skin and soft tissues was evaluated. The implanted scaffold maintained the original shape to some extent (Fig. 8a), and replacement with new (regenerated) bone (NB) was observed in a wide area in the visual field. Furthermore, a circular vacuole region was observed, suggesting the presence of adipocytes (Fig. 8b).

4. Discussion

In this study, the culture period of bone marrow-derived cells was optimized for the bone regeneration in combination with a β-TCP/RCP hybrid scaffold. As a result, bone regeneration was most prominent when bone marrow cells after osteoblast differentiation culture for 7 days was transplanted subcutaneously into mice (Fig. 7). The bone marrow cells with 7 days of osteoblast differentiation culture exhibited the strongest alkaline phosphatase activity and did not form bone matrix (Figs. 3–5). In Real-time RT-PCR, the expression of Runx2, which is a marker of early differentiation, and that of Alp, which is a marker of mid-differentiation, showed the highest values at day 7 among all culture period. These results suggested that the cells subjected to bone differentiation culture for 7 days were a cell population containing relatively immature osteoblasts from the early to middle stages of differentiation [37,38].

One possible explanation for the *in vivo* study results would be the change in cell adhesion ability during differentiation. Cell adhesion has been reported to be involved in osteoblast survival

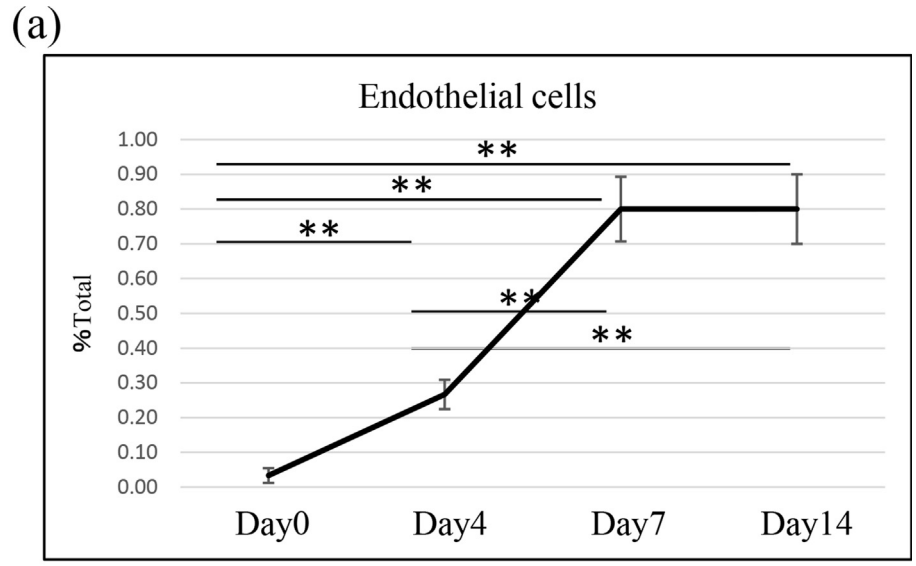

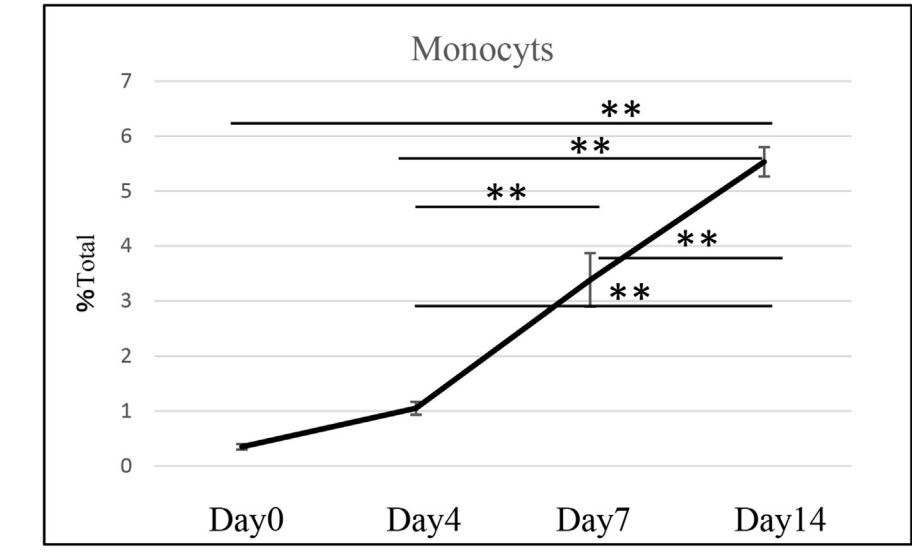

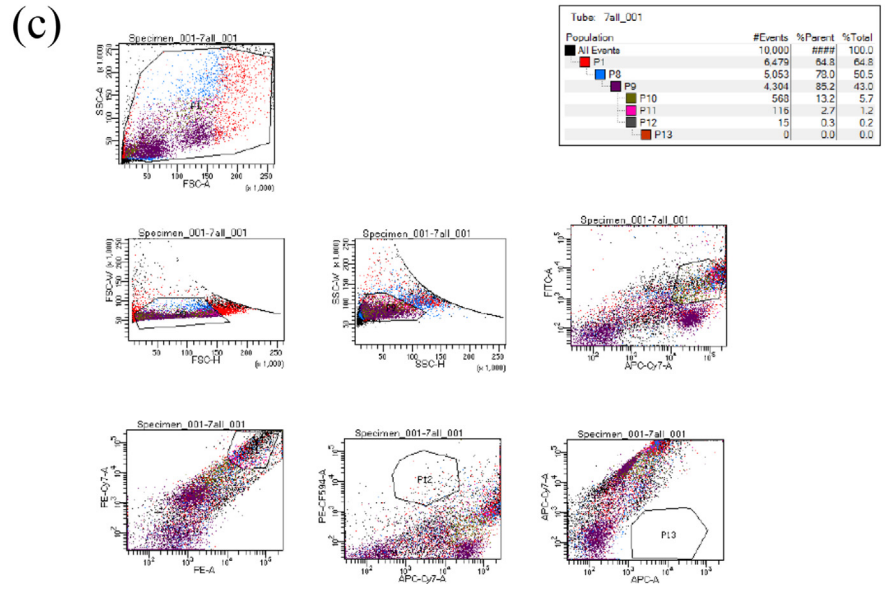

Fig. 6. Changes in% Total of vascular endothelial cells (a) and monocytes (b) in bone marrow cells cultured for different periods of bone. **p < 0.01. Error bars; mean ± S. D. (c) Representative examples of panels used in FACS analysis. P10 is the area of monocytes, and P11 is the area of endothelial cells.

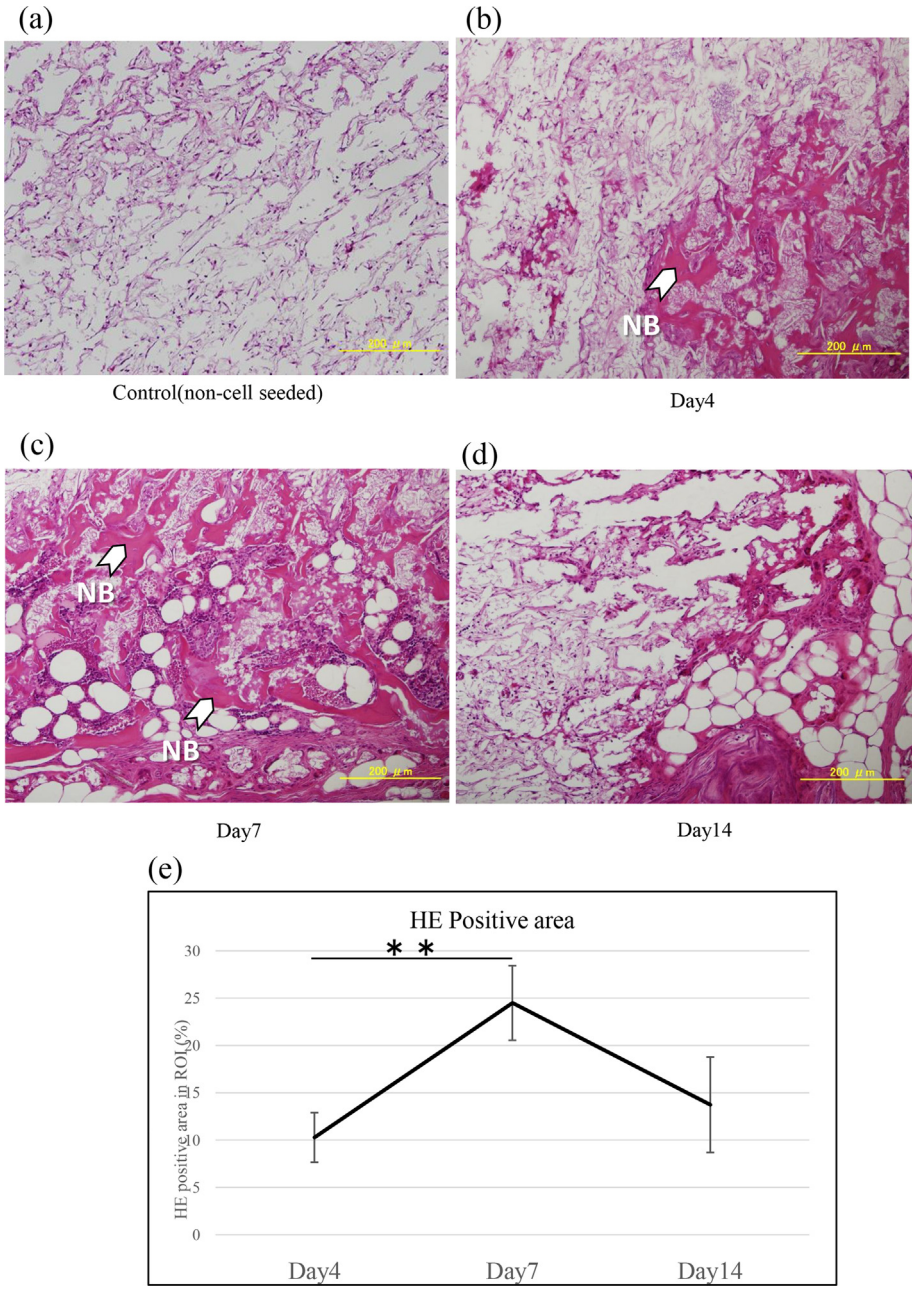

Fig. 7. Histological analysis of harvested tissues by H & E staining. (a): control (the scaffold without cells), (b): the scaffold seeded with cells of 4 days culture, (c): the scaffold seeded with cells of 7 days culture, and (d): the scaffold seeded with cells of 14 days culture. NB: a new (regenerative) bone area. (e)HE-positive areas were quantified using ImageJ. **$p < 0.01$. Error bars; mean ± S. D.

[41]. Compared with immature osteoblast cell lines, osteoblast cell lines at the advanced differentiation stage showed increased cell adhesion, while osteoblast cell lines at the more advanced differentiation stage showed decreased adhesion [42]. It is possible that, in the present study, osteoblasts cultured for 7 days increased cell adhesion and favored bone regeneration, while the 14-day cell culture period decreased adhesion of the cells, which led to ineffective bone formation.

In previous reports, mesenchymal stem cells (MSCs) from bone marrow or adipose tissues were often used in combination with scaffolds [43,44]. In studies using the β-TCP/COL-I hybrid scaffold, MSCs obtained by long-term culture of bone marrow cells were also seeded on the scaffold [27,28]. On the other hand, bone marrow cells cultured for a relatively short time were used in the present study. In the bone marrow, there should be various kinds of cells, such as osteoblasts (and their progenitors), hematopoietic cells (including hematopoietic stem cells), osteoclasts (and their progenitors), MSCs, and vascular endothelial cells. In a previous report, BMP-2 expressed by vascular endothelial cells contained in bone marrow cells was shown to be important for osteoblast differentiation [45]. Another previous report showed that the interaction between hematopoietic stem cells (HSCs) and MSCs is important for angiogenesis, which positively affects the regeneration of bone [46]. It is also indicated that osteoclasts absorb β-TCP and promote bone formation [47]. In this study, the existence ratio of vascular endothelial cells increased significantly up to 7 days, and

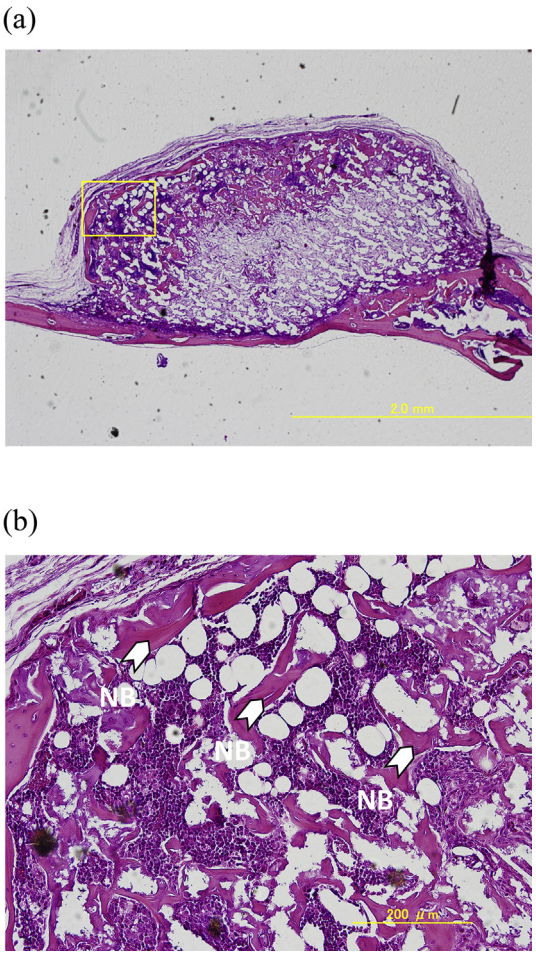

Fig. 8. Histological analysis of harvested tissues by H & E staining. (a): 4x microscope image. (b):20x microscope image. NB: a new (regenerative) bone area. The square in (a) indicates the area in (b).

monocytes increased significantly up to 14 days of culture. These results suggested that the relatively short culture period in the present study resulted in a heterogenous cell population in which interactions of different kinds of cells promoted osteogenesis.

RGD peptide was used for the surface modification of the β-TCP scaffold. The RGD peptide positively affects cell adhesion in vitro, while the effects of RGD on cells *in vivo* are controversial [31,48]. Some previous reports indicated that the RGD motif is important for osteoblast adhesion, improved survival, and bone formation *in vivo* [43]. On the other hand, another report indicated that the RGD motif interfered with cell adhesion *in vivo* [44]. In our study, RCP containing the RGD motif likely promoted the adhesion of cultured bone marrow cells loaded to the scaffold before transplantation, which should have been advantageous for bone regeneration. On the other hand, RCP might have interfered with the adhesion of host cells. To prove the advantage of RCP, a comparison between scaffolds with and without RCP coating should be performed.

In clinical settings, bone augmentation is often performed as a treatment for a hypoplasia of bone in the craniofacial region. To simulate such a situation, the scaffold loaded with cells from 7 days of culture was transplanted onto a calvaria. As a result, bone regeneration occurred while maintaining the shape. In the current bone augmentation using β-TCP, in order to avoid the influence of the pressure of the skin and soft tissues, the transplant is often covered with a titanium mesh. However, there are problems that it needs to be removed by re-operation [49], and the use of metallic materials may cause artifacts in Computed Tomography [50]. The scaffold created in this study was capable of maintaining the shape without metal coverage suggesting the usefulness for the augmentation surgery in clinical practice.

5. Conclusions

In this study, we optimized the culture duration of bone marrow cells before transplantation with a β-TCP/RCP hybrid scaffold. The results suggested that osteoblasts before maturation are important for the most efficient bone regeneration, and the pre-culture period suitable for seeding on a β-TCP/RCP hybrid scaffold is approximately 7 days.

Declaration of interest

The authors declare the following financial interests/personal relationships which may be considered as potential competing interests: Atsuhiko Hikita: Affiliation with an endowed chair from FUJISOFT INCORPORATED.

Acknowledgements

This research was supported by grant in aids from Japan Agency for Medical Research and Development (Research and Development of Advanced Medical Devices and Systems to Achieve the Future of Medicine) and JSPS KAKENHI Grants-in-Aid for Scientific Research (C) (# 18K09806).

We would like to express my gratitude to the people listed below for their various support for research. FUJIFILM Corporation: Michihiro Shibata, Yoshio Ishii and Ai Okamura. CMET Inc.: Makoto Inada. JMC Corporation: Yutaka Sugiura.

References

[1] Zaidi M. Skeletal remodeling in health and disease. Nat Med 2007;13:791–801. https://doi.org/10.1038/nm1593.
[2] Genden EM, Okay D, Stepp MT, Rezaee RP, Mojica JS, Buchbinder D, et al. Comparison of functional and quality-of-life outcomes in patients with and without palatomaxillary reconstruction: a preliminary report. Arch Otolaryngol Head Neck Surg 2003;129:775–80. https://doi.org/10.1001/archotol.129.7.775.
[3] Boyne PJ. Application of bone morphogenetic proteins in the treatment of clinical oral and maxillofacial osseous defects. J Bone Jt Surg 2001;83. https://doi.org/10.2106/00004623-200100002-00009.
[4] JS R, MK H, PN D, GL A. Cysts and cystic lesions of the mandible: clinical and radiologic- histopathologic review. Radiographics 1999;19:1107–24. https://doi.org/10.1148/radiographics.19.5.g99se021107.
[5] Converse JM, Shapiro HH. Bone grafting in malformations of the jaws. Am J Surg 1954;88:858–63. https://doi.org/10.1016/0002-9610(54)90440-7.
[6] Tayapongsak P, O'Brien DA, Monteiro CB, Arceo-Diaz LY. Reconstruction with particulate cancellous bone and marrow. J Oral Maxillofac Surg 1994;52:161–5. https://doi.org/10.1016/0278-2391(94)90401-4.
[7] Shirota T, Ohno K, Motohashi M, Michi KI. Histologic and microradiologic comparison of block and particulate cancellous bone and marrow grafts in reconstructed mandibles being considered for dental implant placement. J Oral Maxillofac Surg 1996;54:15–20. https://doi.org/10.1016/S0278-2391(96)90294-3.
[8] Kitamura M, Akamatsu M, Kawanami M, Furuichi Y, Fujii T, Mori M, et al. Randomized placebo-controlled and controlled non-inferiority phase III trials comparing trafermin, a recombinant human fibroblast growth factor 2, and enamel matrix derivative in periodontal regeneration in intrabony defects. J Bone Miner Res 2016;31:806–14. https://doi.org/10.1002/jbmr.2738.
[9] Hammarström SGSPLL. Emdogain – periodontal regeneration based on biomimicry. Clin Oral Invest 2000:120–5. https://doi.org/10.1007/s007840050127.
[10] Hur Jung-Woo, Yoon Suk-Ja, Ryu Sun-Youl. Comparison of the bone healing capacity of autogenous bone, demineralized freeze dried bone allograft, and collagen sponge in repairing rabbit cranial defects. J Kor Assoc Oral Maxillofac Surg 2012;38:221. jkaoms.2012.38.4.221.
[11] Iwata S, Matsuzaka K, Inoue T. Effects of an atelocollagen sponge during the wound healing of tooth extraction sockets at an early stage. Oral Med Pathol 2010;15:15–20. https://doi.org/10.3353/omp.15.15.

[12] Tanba Jiro. Medical ceramic materials-3. Hydroxyapatite. Jpn j artif Organs 1984;13:1378–82.
[13] Hiroyuki S, Naohiko K, Shinji K, Hiroko T, Toshihiko N, Hiroshi I, et al. Evaluation of hydroxyapatite implants in human periodontal osseous defects. J Jpn Soc Periodontol 1989;31(1):327–33. https://doi.org/10.2329/perio.31.327.
[14] Doi Y, Iwanaga H, Shibutani T, Moriwaki Y, Iwayama Y. Osteoclastic responses to various calcium phosphates in cell cultures. J Biomed Mater Res 1999;47:424–33. https://doi.org/10.1002/(SICI)1097-4636(19991205)47:3<424::AID-JBM19>3.0.CO;2-0.
[15] Xin R, Leng Y, Chen J, Zhang Q. A comparative study of calcium phosphate formation on bioceramics in vitro and in vivo. Biomaterials 2005;26:6477–86. https://doi.org/10.1016/j.biomaterials.2005.04.028.
[16] Bose S, Vahabzadeh S, Bandyopadhyay A. Bone tissue engineering using 3D printing. Mater Today 2013;16:496–504. https://doi.org/10.1016/j.mattod.2013.11.017.
[17] Seitz H, Rieder W, Irsen S, Leukers B, Tille C. Three-dimensional printing of porous ceramic scaffolds for bone tissue engineering. J Biomed Mater Res B Appl Biomater 2005;74:782–8. https://doi.org/10.1002/jbm.b.30291.
[18] Butscher A, Bohner M, Hofmann S, Gauckler L, Müller R. Structural and material approaches to bone tissue engineering in powder-based three-dimensional printing. Acta Biomater 2011;7:907–20. https://doi.org/10.1016/j.actbio.2010.09.039.
[19] Saijo H, Igawa K, Kanno Y, Mori Y, Kondo K, Shimizu K, et al. Maxillofacial reconstruction using custom-made artificial bones fabricated by inkjet printing technology. J Artif Organs 2009;12:200–5. https://doi.org/10.1007/s10047-009-0462-7.
[20] Hikita A, Chung U Il, Hoshi K, Takato T. Bone regenerative medicine in oral and maxillofacial region using a three-dimensional printer. Tissue Eng 2017;23:515–21. https://doi.org/10.1089/ten.tea.2016.0543.
[21] Kanno Y, Nakatsuka T, Saijo H, Fujihara Y, Atsuhiko H, Chung U Il, et al. Computed tomographic evaluation of novel custom-made artificial bones, “CT-bone”, applied for maxillofacial reconstruction. Regen Ther 2016;5:1–8. https://doi.org/10.1016/j.reth.2016.05.002.
[22] Sprio S, Sandri M, Panseri S, Iafisco M, Ruffini A, Minardi S, et al. Bone substitutes based on biomineralization. Woodhead Publishing Limited; 2014. https://doi.org/10.1533/9780857099037.1.3.
[23] Kon E, Delcogliano M, Filardo G, Fini M, Giavaresi G, Francioli S, et al. Orderly osteochondral regeneration in a sheep model using a novel nano-composite multilayered biomaterial. J Orthop Res 2010;28:116–24. https://doi.org/10.1002/jor.20958.
[24] Tampieri A, Celotti G, Landi E, Sandri M, Roveri N, Falini G. Biologically inspired synthesis of bone-like composite: self-assembled collagen fibers/hydroxyapatite nanocrystals. J Biomed Mater Res 2003;67:618–25. https://doi.org/10.1002/jbm.a.10039.
[25] Lee MH, You C, Kim KH. Combined effect of a microporous layer and type I collagen coating on a biphasic calcium phosphate scaffold for bone tissue engineering. Materials 2015;8:1150–61. https://doi.org/10.3390/ma8031150.
[26] Arahira T, Todo M. Variation of mechanical behavior of β-TCP/collagen two phase composite scaffold with mesenchymal stem cell in vitro. J Mech Behav Biomed Mater 2016;61:464–74. https://doi.org/10.1016/j.jmbbm.2016.04.019.
[27] Lin J, Shao J, Juan L, Yu W, Song X, Liu P, et al. Enhancing bone regeneration by combining mesenchymal stem cell sheets with β-TCP/COL-I scaffolds. J Biomed Mater Res B Appl Biomater 2018;106:2037–45. https://doi.org/10.1002/jbm.b.34003.
[28] Baheiraei N, Nourani MR, Mortazavi SMJ, Movahedin M, Eyni H, Bagheri F, et al. Development of a bioactive porous collagen/β-tricalcium phosphate bone graft assisting rapid vascularization for bone tissue engineering applications. J Biomed Mater Res 2018;106:73–85. https://doi.org/10.1002/jbm.a.36207.
[29] Luo T, Kiick KL. Collagen-like peptides and peptide-polymer conjugates in the design of assembled materials. Eur Polym J 2013;49:2998–3009. https://doi.org/10.1016/j.eurpolymj.2013.05.013.
[30] García AJ. Get a grip: integrins in cell-biomaterial interactions. Biomaterials 2005;26:7525–9. https://doi.org/10.1016/j.biomaterials.2005.05.029.
[31] Wang C, Liu Y, Fan Y, Li X. The use of bioactive peptides to modify materials for bone tissue repair. Regen Biomater 2017;4:191–206. https://doi.org/10.1093/rb/rbx011.
[32] Confalonieri D, La Marca M, van Dongen EMWM, Walles H, Ehlicke F. * an injectable recombinant collagen I peptide-based macroporous microcarrier allows superior expansion of C2C12 and human bone marrow-derived mesenchymal stromal cells and supports deposition of mineralized matrix. Tissue Eng 2017;23:946–57. https://doi.org/10.1089/ten.TEA.2016.0436.
[33] Olsen D, Yang C, Bodo M, Chang R, Leigh S, Baez J, et al. Recombinant collagen and gelatin for drug delivery. Adv Drug Deliv Rev 2003;55:1547–67. https://doi.org/10.1016/j.addr.2003.08.008.
[34] Brittberg M, Lindahl A. Tissue engineering of cartilagevol. 249; 2008. https://doi.org/10.1016/B978-0-12-370869-4.00018-5.
[35] Abramoff MD, Magalhaes PJ, Ram SJ. Image processing with ImageJ. Biophot Int 2004;11(7):36–42.
[36] Schneider CA, Rasband WS, Eliceiri KW, Instrumentation C. NIH image to ImageJ : 25 years of image. Analysis 2017;9:671–5.
[37] Miron RJ, Zhang YF. Osteoinduction: a review of old concepts with new standards. J Dent Res 2012;91:736–44. https://doi.org/10.1177/0022034511435260.
[38] Tang Z, Li X, Tan Y, Fan H, Zhang X. The material and biological characteristics of osteoinductive calcium phosphate ceramics. Regen Biomater 2018;5:43–59. https://doi.org/10.1093/rb/rbx024.
[39] Wang H, Wang S, Ye J, Yin Y, Zhou Y, Ma X, et al. Enumeration of monocytes subsets using different gating methods by flow cytometry. Int J Clin Exp Pathol 2016;9:1285–93.
[40] Cochrane A, Kelaini S, Tsifaki M, Bojdo J, Vila-Gonzalez M, Drehmer D, et al. Quaking is a key regulator of endothelial cell. Stem Cell 2017;35:952–66.
[41] Moioli EK, Clark PA, Chen M, Dennis JE, Erickson HP, Gerson SL, et al. Synergistic actions of hematopoietic and mesenchymal stem/progenitor cells in vascularizing bioengineered tissues. PloS One 2008;3. https://doi.org/10.1371/journal.pone.0003922.
[42] Benayahu D, Fried A, Efraty M, Robey PC, Wientroub S. Bone marrow Interface : preferential attachment of an osteoblastic marrow stromal cell line. J Cell Biochem 1995;59:151–60. https://doi.org/10.1002/jcb.240590204.
[43] Baba S, Inoue T, Hashimoto Y, Kimura D, Ueda M, Sakai K, et al. Effectiveness of scaffolds with pre-seeded mesenchymal stem cells in bone regeneration - assessment of osteogenic ability of scaffolds implanted under the periosteum of the cranial bone of rats-. Dent Mater J 2010;29:673–81. https://doi.org/10.4012/dmj.2009-123.
[44] Yoon E, Dhar S, Chun DE, Gharibjanian NA, Evans GRD. In vivo osteogenic potential of human adipose-derived stem cells/poly lactide-co-glycolic acid constructs for bone regeneration in a rat critical-sized calvarial defect model. Tissue Eng 2007;13:619–27. https://doi.org/10.1089/ten.2006.0102.
[45] Kaigler D, Krebsbach PH, West ER, Horger K, Huang YC, Mooney DJ. Endothelial cell modulation of bone marrow stromal cell osteogenic potential. Faseb J 2005;19:665–7. https://doi.org/10.1096/fj.04-2529fje.
[46] Marom R, Shur I, Solomon R, Benayahu D. Characterization of adhesion and differentiation markers of osteogenic marrow stromal cells. J Cell Physiol 2005;202:41–8. https://doi.org/10.1002/jcp.20109.
[47] Yukiko O, Naoya I, Michiko Y, Chikara S. Histological study of bone formation associated with the implantation of bone marrow cells/porous beta-TCP block composites. Jpn J Oral Surg 2007;53:468–80. https://doi.org/10.5794/jjoms.53.468.
[48] Mork BC DP, Vitebsky A, Hou M, Preising B. Advantages of RGD peptides for directing cell association with biomaterials. J Biomater 2008;32:2–5. https://doi.org/10.1016/j.biomaterials.2011.02.029.Advantages.
[49] Mitsuyoshi I, Masayuki F, Hirokazu N, Takayoshi O, Kaoru Y, Shinichi T. Mandibular reconstruction of large bone defects by using titanium mesh and particulate cancellous bone and marrow harvested from bilateral posterior iliac crests. J Jpn Stomatol Soc 2003;52:253–60. https://doi.org/10.11277/stomatology1952.52.253.
[50] Masato T, Tadashi T, Haruhiko I, Shinya T, Mutsuo A, Kazuo K. Reconstruction of Orbital floor following total Maxillectomy use of Titanium mesh and free forearm flap. Jpn J Head Neck Cancer 1996;22:49–53. https://doi.org/10.5981/jjhnc1974.22.49.